

An Experimental and Computational Study of 2-(3-Oxo-3H-benzo[f] chromen-1-ylmethoxy)-Benzoic Acid Methyl Ester

C. G. Renuka¹ · K. Shivashankar² · P. Boregowda² · S. S. Bellad³ · M. V. Muregendrappa⁴ · Y. F. Nadaf³

Received: 22 August 2016 / Accepted: 15 May 2017 / Published online: 8 August 2017
© Springer Science+Business Media, LLC 2017

Abstract The various methods for studying polarities are based on the use of probe molecules, whose molecular spectral profile is significantly affected by the polarity of the medium. The absorption and emission spectra and dipole moments (μ_g and μ_e) of 2-(3-oxo-3H-benzo[f]chromen-1-ylmethoxy)-benzoic acid methyl ester (2BME) are studied in solvents of different polarities at room temperature. The determination of dipole moments by solvatochromic shift using various relations and the change in dipole moment ($\Delta\mu$) were determined using Stokes shift with the variation of the solvent polarity parameter (E_T^N). The value of μ_e greater than μ_g indicating that the probe is more polar in the higher state. DFT and TDDFT theoretical analysis of dipole moment in the vacuum and with solvent, solvent accessible surface (SAS) and molecular electrostatic potential (MEP) are also performed.

Keywords Solvatochromic method · Polarity function · Dipole moments · DFT calculations · HOMO–LUMO

1 Introduction

Coumarin and its derivatives [1] have attracted considerable attention in recent years for their versatile properties in chemistry and pharmacology. The 3-carboxamide coumarins [2] have been described as small molecular weight FXIIa inhibitors. Synthetic coumarins

✉ Y. F. Nadaf
dryfnadaf@gmail.com

¹ P.G. Department of Physics, Jnanabharathi campus, Bangalore University, Bengaluru 560056, India

² P.G. Department of Chemistry, Central College Campus, Bangalore University, Bengaluru 560001, India

³ Department of Physics and Research Center, Maharani Science College for Women, Bengaluru 560056, India

⁴ Department of Physics, BMSIT Basavanagudi, Bengaluru 560056, India

[3] have been found to be active against the pancreatic cancers. These natural coumarins [4] isolated from *Angelica decursiva* and *Artemisia capillaris* have shown anti-Alzheimer's disease factors. Coumarins [5] which have been isolated from roots of *Angelica dahurica* cv. Hangbaizhi showed significant anti-inflammatory action; coumarins have some ability to regulate the diverse range of cellular pathways useful for some anticancer treatments [6]. Drug–metal interactions have been used to develop highly sensitive biosensors for bacteria [7, 8].

The excited state dipole moment determination using the Lippert–Mataga equation is adopted widely [9]; in this method, absorption and emission shifts, dielectric constant (ϵ) and the refractive index (n) are used. Ground (μ_g) and excited (μ_e) state dipole moments of a probe vary due to changes in the polarity or dielectric constant of the solvent, which leads to variations in μ_g and μ_e . Analysis of the effect of solvent gives more information and is very useful in studying μ_e of the molecule. These studies are helpful in designing non-linear optical devices [10], probing the nature of photochemical transformations and the calculation of molecular polarizability [11]. The empirical results for μ_e are also helpful for quantum chemical (QC) analysis.

We have studied the μ_g and μ_e of exalites [12, 13] and coumarin laser dyes [14, 15] using Guggenheim's and solvatochromic shift methods. These methods which were reported [13–15] a decade ago have been adopted by many researchers. Several research groups have made empirical and theoretical consideration on μ_g and μ_e using various methods on organic molecules like coumarin [16], ketocyanine dye [17] and others [18–24].

It is known that the position of the bands of a probe in solutions varies due to specific and nonspecific interactions with the probe. The solvent induced spectral shift of a probe is difficult to understand because of the difficulty with the theoretical definition of the solvent polarity; for this reason different solvent polarity parameters and scales are used. Density functional theory (DFT) using the B3LYP functional and 6-311 basis set method was used to study the hydrogen bond by considering the difference between the structures with and without the bond; DFT predicts structural properties, lowest energy of the probe in gas phase and in the solvent.

In the present context, the photophysical properties of the 2BME molecule have been studied in different solvents of varying polarity and hydrogen bonding characteristics. The Stokes data of 2BME is used to determine μ_e values of the singlet form, which have been verified using Lippert and Mataga bulk solvent functions [25, 26] given by Kamlet et al. [27–29]. The μ_g of 2BME was determined by the QC method and μ_e was measured using Lippert–Mataga (LME), Bakshiev's (BE) [30], Kawski–Chamma–Viallet's (KCVE) and McRae (McRE) [31–36] relations and an equation based on Reichardt's microscopic solvent polarity parameter E_T^N [37]. The QC parameters have been adapted to analyze dipole moment, HOMO, LUMO, MEP and SAS of 2BME in vacuum and in ethanol as solvent [38].

2 Materials and Methods

2.1 Materials

The synthesis of 2-(3-oxo-3H-benzo[f]chromen-1-ylmethoxy)-benzoic acid methyl ester (2BME) was carried out by standard methods (Fig. 1) with a 97% yield [39].

Spectroscopic grade (SD Fine Chem. Ltd. India) solvents: acetone, ethanol, ethyl acetate, hexane, methanol, *N,N*-dimethylformamide (*N,N*-DMF), tetrahydrofuran, propanol, chloroform and butyl acetate, having 99% purity, were used without further purification. The concentrations of 2BME solutions were 10^{-4} – 10^{-5} mol·dm $^{-3}$. Dielectric constants (ϵ) and refractive indices (n) of the solvents obtained from the literature [40–43] are presented in the Table 1.

2.2 Experimental Methods

UV–vis absorption spectra (Shimadzu UV-1800 spectrophotometer) over a wavelength range of 200–800 nm and steady-state fluorescence spectra were obtained (Hitachi F-2700 Fluorescence Spectrophotometer) by selecting excitation wavelengths 319 and 347 nm. The measurements were carried out using 1.0×1.0 cm quartz cell sample holder, all the experimental measurements were done at 27.00 °C.

2.3 Theoretical Background

From the literature, [12–15] the determination of the excited state dipole moments of different molecules by the solvatochromic shift method, using different assumptions, results in four independent equations for the estimation of the μ_e for 2BME as follows:

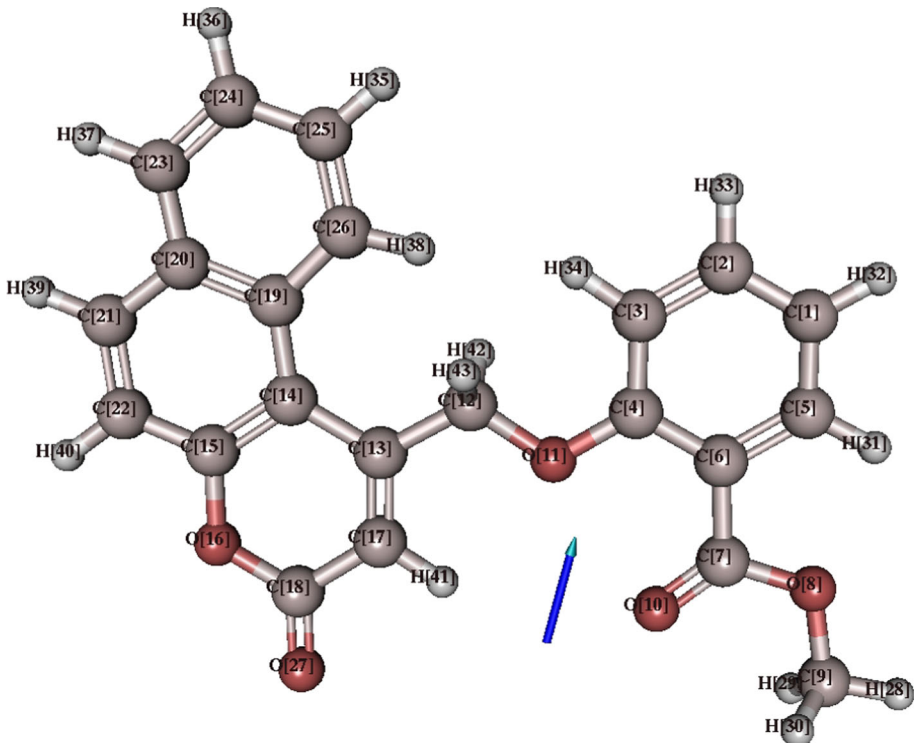


Fig. 1 Optimized molecular structure and direction of the dipole moment of the 2BME molecule

Table 1 Values of solvent polarity parameters

Solvent	ϵ	n	$F_1(\epsilon, n)$	$F_2(\epsilon, n)$	$F_3(\epsilon, n)$	$F_4(\epsilon)$	$E_T(30)$	E_T^N	α	β	π^*
Hexane	1.89	1.38	-8.45×10^{-5}	1×10^{-3}	0.25	0.45	39.1	0.0093	–	–	–0.01
Chloroform	2.21	1.45	0.15	0.37	0.55	0.57	36.0	0.26	0.20	0.1	0.69
Ethyl acetate	6.02	1.37	0.19	0.48	0.49	1.25	38.5	0.22	0.00	0.45	0.45
Butyl acetate	6.17	1.37	0.20	0.49	0.56	1.26	50.3	0.24	–	0.45	–
Tetrahydrofuran	7.58	1.41	0.21	0.55	0.61	1.37	42.2	0.21	–	0.55	0.55
Acetone	20.7	1.36	0.24	0.79	0.96	1.73	50.7	0.35	0.08	0.43	0.71
Propanol	20.8	1.39	0.27	0.78	0.65	1.73	51.9	0.61	0.84	0.90	0.52
Ethanol	25.3	1.36	0.28	0.81	0.65	1.82	55.4	0.65	0.83	0.77	0.54
Methanol	33.0	1.33	0.30	0.85	0.65	1.84	43.2	0.76	0.98	0.66	0.60
<i>N,N</i> DMF	36.71	1.43	0.27	0.84	0.77	1.85	–	0.40	0.00	0.69	0.88

Lipper–Mataga equation [44]

$$\tilde{\nu}_a - \tilde{\nu}_f = m_1 F_1(\varepsilon, n) + \text{constant} \tag{1}$$

where $\tilde{\nu}_a$ and $\tilde{\nu}_f$ are the absorption and fluorescence maxima and

$$F_1(\varepsilon, n) = \frac{\varepsilon - 1}{2\varepsilon + 1} \frac{n^2 - 1}{2n^2 + 1}.$$

Bakshiev’s equation [45]

$$\tilde{\nu}_a - \tilde{\nu}_f = m_2 F_2(\varepsilon, n) + \text{constant} \tag{2}$$

where $F_2(\varepsilon, n) = \frac{2n^2+1}{n^2+2} \left[\frac{\varepsilon-1}{\varepsilon+2} - \frac{n^2-1}{n^2+2} \right]$.

Kawski–Chamma–Viallet equation [46]

$$\frac{\tilde{\nu}_a + \tilde{\nu}_f}{2} = m_3 F_3(\varepsilon, n) + \text{constant} \tag{3}$$

where $F_3(\varepsilon, n) = \left[\frac{2n^2+1}{2(n^2+2)} \left(\frac{\varepsilon-1}{\varepsilon+2} - \frac{n^2-1}{n^2+2} \right) + \frac{3(n^4-1)}{2(n^2+2)^2} \right]$.

McRae equation [47]

$$\tilde{\nu}_a = -m_4 F_4(\varepsilon) + \text{constant} \tag{4}$$

where $F_4(\varepsilon) = \left[\frac{2(\varepsilon-1)}{\varepsilon+2} \right]$.

The above equations use quantum mechanical perturbation theory for $\tilde{\nu}_a$, $\tilde{\nu}_f$ and Stokes shifts in various solvents, where:

$$m_1 = \frac{2(\mu_e - \mu_g)^2}{hca^3} \tag{5}$$

$$m_2 = \frac{2(\mu_e - \mu_g)^2}{hca^3} \tag{6}$$

$$m_3 = \frac{2(\mu_e^2 - \mu_g^2)}{hca^3} \tag{7}$$

$$m_4 = \frac{\mu_g(\mu_e - \mu_g)}{hca^3} \tag{8}$$

where c is the velocity of light in vacuum and h is Planck’s constant. The m_1, m_2, m_3 and m_4 are the slopes of the plots of (1) $(\tilde{\nu}_a - \tilde{\nu}_f)$ against $F_1(\varepsilon, n)$, (2) $(\tilde{\nu}_a - \tilde{\nu}_f)$ against $F_2(\varepsilon, n)$, (3) $\left(\frac{\tilde{\nu}_a + \tilde{\nu}_f}{2}\right)$ against $F_3(\varepsilon, n)$ and (4) $\tilde{\nu}_a$ against $F_4(\varepsilon)$, respectively. The Onsager radius, a , of a solute molecule was estimated according to the Edward atomic increment method [48]. If the μ_g and μ_e dipole moments are parallel, then:

$$\mu_g = \frac{m_3 - m_2}{2} \left[\frac{hca^3}{2m_1} \right]^{\frac{1}{2}} \tag{9}$$

$$\mu_e = \frac{m_3 + m_2}{2} \left[\frac{hca^3}{2m_1} \right]^{\frac{1}{2}} \quad (10)$$

$$\mu_e = \left[\frac{m_3 + m_2}{m_3 - m_2} \right] \mu_g ; m_3 > m_2. \quad (11)$$

If the μ_g and μ_e are non-parallel, forming an angle φ , then φ can be estimated using the formula:

$$\cos \varphi = \frac{1}{2\mu_g\mu_e} \left[(\mu_e^2 + \mu_g^2) - \frac{m_3}{m_2} (\mu_e^2 - \mu_g^2) \right] \quad (12)$$

The slopes are m_1 , m_2 and m_3 and are obtained by plotting $(\tilde{\nu}_a - \tilde{\nu}_f)$ and $(\frac{\tilde{\nu}_a - \tilde{\nu}_f}{2})$ against solvent polarity functions.

2.3.1 Molecular Microscopic Solvent Polarity Parameter E_T^N

Reichardt gave [49] the polarity parameter E_T^N and using this the excited state dipole moment of a molecule can be calculated as:

$$\tilde{\nu}_a - \tilde{\nu}_f = 11307.6 \left[\left(\frac{\delta\mu}{\delta\mu_B} \right)^2 \left(\frac{a_B}{a} \right)^3 \right] E_T^N + \text{constant} \quad (13)$$

where $\delta\mu_B$ is the variation in dipole moment and a_B the Onsager radius of the betaine molecule and $\delta\mu$ and a the values for the solute molecule being studied. The value of $\delta\mu$ can be determined as:

$$\delta\mu = \mu_e - \mu_g = \sqrt{\frac{81m}{11307.6(6.2/a)^3}} \quad (14)$$

where m is the slope of linear plot of Stoke shift against E_T^N .

2.3.2 Kamlet–Taft Solvatochromic Parameters

The multiparametric approach was proposed by Kamlet and co-workers [50]. The magnitude of solute–solvent interactions are estimated using a solvatochromic method. The solvent effect on some measurable property A is assumed to be linearly dependent on three parameters of the medium: the polarizability parameter π^* , the hydrogen bond donor (HBD) parameter α , and hydrogen bond acceptor parameter β . The effect of the solvent on the absorption, A , is expressed by the generalized equation:

$$A = A_0 + s\pi^* + a\alpha + b\beta \quad (15)$$

where A_0 is the vapor phase wavenumber and the values of A are spectral band maxima in the different media. The Kamlet–Taft coefficients, s , a and b give the relative sensitivities of A to the individual parameters.

2.4 Computational Details

The theoretical simulations using the Gamess [51] and optimization of geometry was done with DFT with the B3LYP functional and 6-311 (d,p) basis set. The vertical excitations, density graph and optimization of the μ_g were analyzed with the help of TDDFT (time-dependent DFT) at the B3LYP/6-311 (d,p) level. The HOMO and LUMO were calculated in vacuum and in ethanol as solvent.

3 Results and Discussion

3.1 Effect Solvent on Absorption and Fluorescence Spectra

Absorption (Fig. 2) and fluorescence (Fig. 3) studies were done for the 2BME molecule at room temperature. The absorption peak of 2BME varies from 231 to 348 nm in solvent medium which leads to π - π^* transition. The Stokes shifts values in different solvents indicate μ_g of the sample in protic solvents.

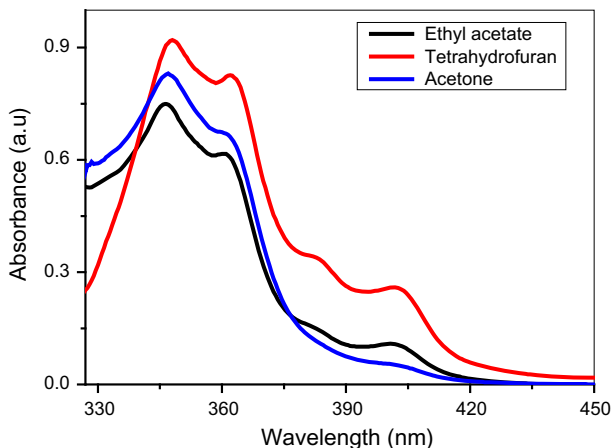
The fluorescence spectra of 2BME is red-shifted between 285 and 427 nm from hexane to *N,N*-DMF. The effect of solvent on the fluorescence emission is much greater than on the absorption maximum. These results suggest that the ground state is less polar than the higher emission state [52–54]. The linearity between the $E_T(30)$ and the Stokes shift was analyzed. The molecule 2BME show increases in Stokes shift from aprotic to protic medium due to increase in the solvent polarity and intramolecular charge transfer state (ICT).

The nature of 2BME molecule in solvents with various polarities may be explored using the differences in μ_g and μ_e . The charge separation on electronic excitation of 2BME is measured by analyzing the change dipole moment ($\Delta\mu = \mu_e - \mu_g$). According to Lippert–Mataga (Eq. 1) [55]:

$$\Delta\tilde{\nu} = \tilde{\nu}_a - \tilde{\nu}_f = \left[\frac{2(\mu_e - \mu_g)}{hca^3} \right] F_1(\epsilon, n) + \text{constant} \quad (16)$$

where $F_1(\epsilon, n) = \frac{\epsilon-1}{2\epsilon+1} \frac{n^2-1}{2n^2+1}$, which shows the orientation polarizability and polarity parameter of the solvent; Fig. 4 represents the Lippert–Mataga linear plot for various solvents.

Fig. 2 Absorption spectra of 2BME in different solvents



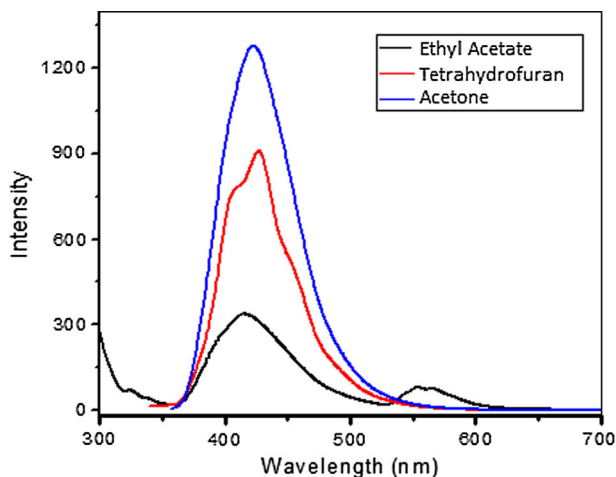


Fig. 3 Fluorescence spectra of 2BME in different solvents

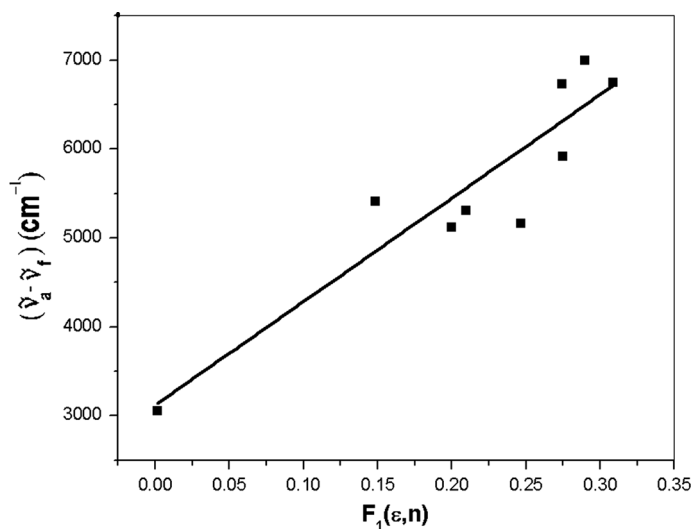


Fig. 4 Plot of Stokes shift versus solvent polarity function $F_1(\epsilon, n)$ using the Lippert equation for 2BME

The linear plots of the Bakshiev and Chamma–Viallet equations, $E_T(30)$ against $(\tilde{\nu}_a - \tilde{\nu}_f)$, E_T^N against $(\tilde{\nu}_a - \tilde{\nu}_f)$ and the McRae equation are shown in Figs. 5, 6, 7, 8 and 9.

The Kamlet and Taft [56] method was used to explore the effects of the various modes of solvation on the absorption and fluorescent energies. The parameters π^* , α and β are used to characterize the polarizability and to describe the respective properties of a given solvent in Eq. 15. Table 2 lists the absorption and emission bands of 2BME. The solvent dipolar interaction (π^*) (Table 1) and hydrogen bond accepting property (β) are the principal parameters which lead to the stabilization of the μ_g and μ_e of the 2BME molecule.

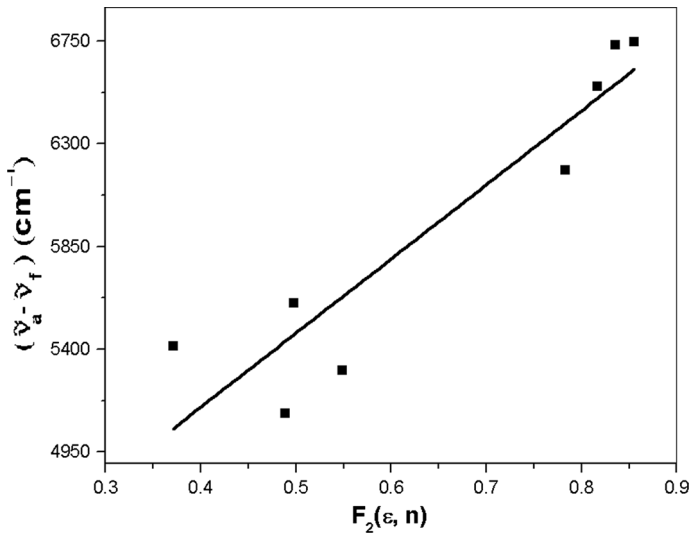


Fig. 5 Plot of Stokes shift versus solvent polarity function $F_2(\epsilon, n)$ using the Bakshiev equation for 2BME

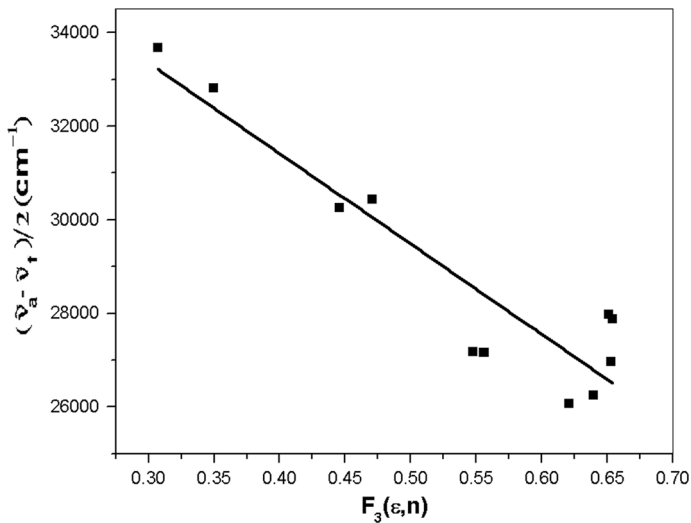


Fig. 6 Plot of Stokes shift versus solvent polarity function $F_3(\epsilon, n)$ using Kawski–Chamma–Villet's equation for 2BME

3.2 Estimation of Dipole Moments

The solvent parameters, solvent functions (Table 1) and values of μ_g and μ_c of 2BME are determined using Eqs. 1–4 as shown in Table 2.

Plots of $(\tilde{\nu}_a - \tilde{\nu}_f)$ against $F_1(\epsilon, n)$, $(\tilde{\nu}_a - \tilde{\nu}_f)$ against $F_2(\epsilon, n)$, $(\tilde{\nu}_a - \tilde{\nu}_f)/2$ against $F_3(\epsilon, n)$, $(\tilde{\nu}_a - \tilde{\nu}_f)$ against E_T^N , $\tilde{\nu}_a$ against $F_4(\epsilon)$ and $(\tilde{\nu}_a - \tilde{\nu}_f)$ against $E_T(30)$ are shown in Figs. 4, 5, 6, 7, 8 and 9 and the intercepts, slopes and correlation coefficients are shown in Table 3.

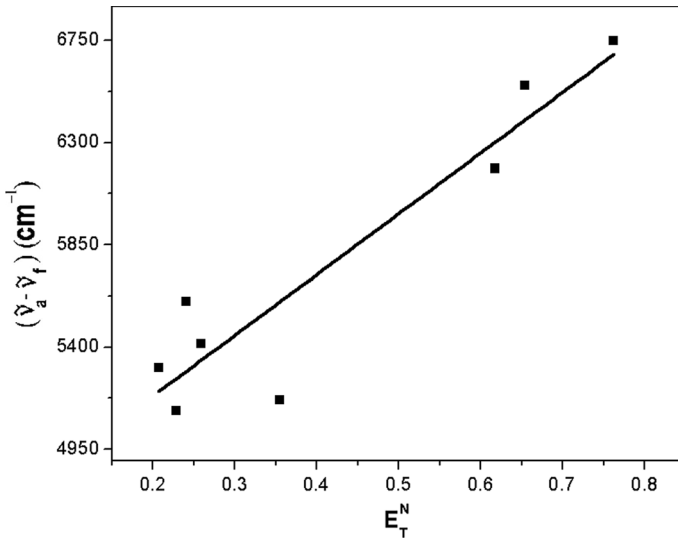


Fig. 7 Plot of Stokes shift versus solvent polarity function E_T^N using the Reichardt equation for 2BME

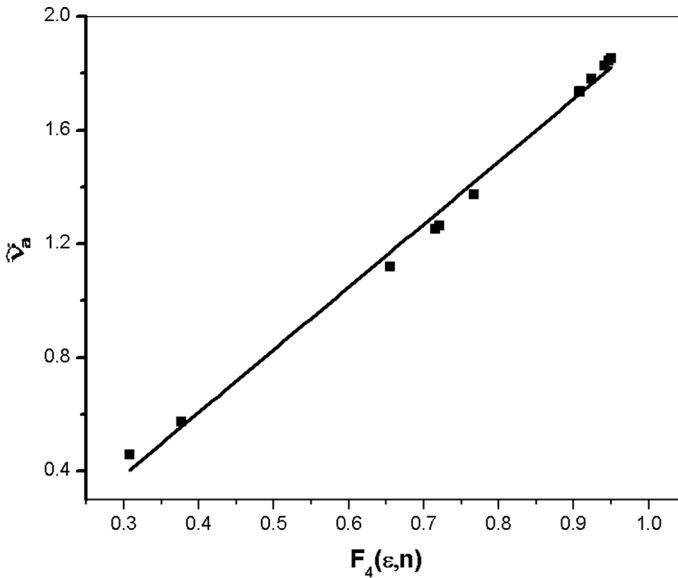


Fig. 8 Plot of Stokes shift versus solvent polarity function $F_4(\epsilon, n)$ using the McRae equation for 2BME

The plots are linear for eight solvents while other points varied from linearity due to specific solute–solvent interactions.

From Table 3, the r values vary from 0.8162 to 0.9933 depending on the solvents used, which represents the linearity for these correlations. The linear behavior of the Stokes shifts versus solvent polarity function indicates general solvent effects as a function of dielectric constant and refractive index. The Onsager cavity radii of 2BME was measured

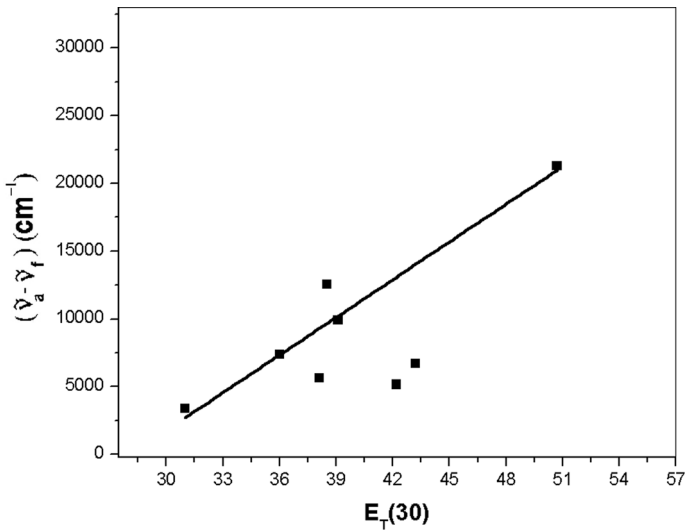


Fig. 9 Plot of Stokes shift versus solvent polarity function $E_T(30)$ for 2BME

Table 2 Experimental absorption and fluorescence properties of 2BME in different solutions

Solvent	λ_a (nm)	λ_c (nm)	$\tilde{\nu}_a$ (cm^{-1})	$\tilde{\nu}_f$ (cm^{-1})	$\tilde{\nu}_a - \tilde{\nu}_f$ (cm^{-1})
Hexane	262	285.0	38138.8	35087.7	3051.1
Chloroform	304	417.5	32954.4	23952.1	9002.3
Ethyl acetate	347	421.5	28843.4	23724.8	5118.6
Butyl acetate	270	419.7	37064.1	23821.3	13243.0
Tetrahydrofuran	348	427.0	28727.4	23419.2	5308.2
Acetone	347	422.5	28835.1	23668.6	5166.4
Propanol	231	416.0	43384.0	24038.5	19345
Ethanol	268	411.0	37369.2	24330.9	13038
Methanol	319	356.0	31348.0	28089.9	3258.1
<i>N,N</i> DMF	269	328.5	37174.7	30441.4	6733.3

Table 3 Statistical treatment of the correlations of the spectral shift of 2BME

Equations of the form equation	Slope (m)	Intercept	Correlation coefficient (r)	No. of data
Lippert–Mataga correlation	$m_1 = 11637.97$	3122.72	0.8162	10
Bakhshieve correlation	$m_2 = 3248.76$	3846.29	0.8370	8
Kawski–Chamma–Viallet	$m_3 = 19311.13$	39140.0	0.8447	11
E_T^N correlation	$m_4 = 2673.746$	4650.57	0.8562	8
McRae	$m_5 = 2.20695$	-0.27577	0.9933	12
$E_{T(30)}$	$m_6 = 843.25$	4650.57	0.863	8

by the atomic increment method and found to be 4.16 Å. The ground state dipole moment is determined from the m_2 and m_3 slopes of the BE and KCVE methods, using Eqs. 6 and 7 and also the μ_e values are obtained from m_1 , m_2 , m_3 and m_4 of LME, BE, KCVE, MRE and E_T^N by applying Eqs. 9, 10 and 14 and the results are presented in Table 4.

Table 4 indicates that μ_e (2.553 D) is found to be 1.13 times larger than μ_g (2.266 D). μ_g ; differences are in the range of 2.411–7.0871 D, which shows that the molecule is more polar in the excited state than in the ground state. The differences between μ_g and μ_e can give the properties of the emitting state, charge transfer and change occurring under excitation. The μ_e value of 7.0878 D obtained from BE is higher than the values from the other equations. The angle between the μ_g and μ_e vectors calculating using Eq. 12 is found to be 9.236°, its direction depends on the center of charges. The small change in angle results in the higher charge distribution across the molecule in the excited state.

The linear correlation values are greater than 0.8 (Table 3), which gives linearity of the Stokes shift; the deviations from linearity could be from solute–solvent interactions. For the 2BME molecule the interaction with nonpolar solvents is due to the dipole–induced dipole interactions, the solute–solvent interaction depend on the higher dipole–dipole interactions (also pointed out by others [57, 58]) to use E_T (30) parameter, which is the experimental solvent parameter [43] for the polarization dependent spectral behavior. However, $E_T(30)$ data have dimensions of $\text{kJ}\cdot\text{mol}^{-1}$ [40]; hence, the normalized E_T^N data has been considered. The μ_g analysis by the B3LYP/6-311 (d,p), PCM and SCF techniques

Table 4 Ground state and singlet excited state dipole moments of 2BME in Debye (D)

Compound	2BME
Onsager radius Å	4.160
μ_g^a (D)	2.266
μ_e^b (D)	2.553
μ_e^c (D)	7.087
μ_e^d (D)	2.496
μ_e^e (D)	4.397
μ_e^f (D)	2.411
$\Delta\mu_e^g$ (D)	0.286
$\frac{\mu_e^h}{\mu_g}$ (D)	0.887
$\Delta\mu_e^i$ (D)	2.405
φ^j (rad)	0.161

^a Ground state dipole moment from quantum chemical calculation

^b Excited state dipole moment calculated from the Kawski–Chamma–Viallet equation

^c Excited state dipole moment calculated from the Bakhshiev equation

^d Excited state dipole moment calculated from the Lippert–Mataga equation

^e Excited state dipole moment calculated from the E_T^N equation

^f Excited state dipole moment calculated from the McRae equation

^g Change in dipole moments from μ_e and μ_g

^h The ratio of excited state and ground dipole moments

ⁱ The difference in ground state and excited dipole using the E_T^N method

^j The orientation of the molecule in excited state relative to the ground state

are obtained as 2.203 D (vacuum), and 2.269 D (ethanol), respectively. The empirical and the theoretical results vary because theoretical analysis is for the isolated gaseous molecule and the empirical values are in the solid-state.

3.2.1 Molecular–Microscopic Solvent Polarity Parameter (E_T^N)

The graph of Stoke's shift of 2BME against E_T^N values for various media is shown in Fig. 7. The μ_e value calculated using E_T^N according to Eq. 13 is given in Table 4. The μ_e value 4.397 D by the E_T^N method is 46.85% smaller than that from the Bakhshiev method. This is because BE does not consider specific solute solvent interaction while these details are included in the technique based on E_T^N [37]. The increasing in solvent polarity in UV–vis and fluorescence bands give a bathochromic shift. This shows the ICT absorption of the less dipolar μ_g molecule with dominant mesomeric structure results in greater dipolarity in μ_e of the molecule with prominent structure. Hence, the μ_e for 2BME is more polar than the μ_g state due to ICT.

3.2.2 Kamlet–Taft Solvatochromic Parameters

For explaining the solvent polarity dependence and hydrogen bonding ability of 2BME, the analysis used the Kamlet–Taft equation, which takes account of the polarity and hydrogen bond ability of the solvents. To HBD and HBA abilities of $\tilde{\nu}_a$, $\tilde{\nu}_f$ and $\Delta\tilde{\nu} = (\tilde{\nu}_a - \tilde{\nu}_f)$ are related to α , β and π^* by multiple regression. This analysis results along with (r) are presented in the below relations:

$$\tilde{\nu}_a(\text{cm}^{-1}) = 38046.29 - 3426.01\pi^* + 7851.22\alpha + 7263.5\beta \quad (r = 0.957)$$

$$\tilde{\nu}_f(\text{cm}^{-1}) = 24267.68 + 1152.4\pi^* + 712.315\alpha + 640.714\beta \quad (r = 0.819)$$

$$\Delta\tilde{\nu}(\text{cm}^{-1}) = 3163.67 + 7865.0\pi^* - 1657.10\alpha + 6422.16\beta \quad (r = 0.813).$$

The absorption and emission spectra (ν_{max}) values vary and the polarizability parameter (s) increases from μ_g to μ_e , which gives the stability of the molecule. It can be concluded from the above relations that the non-specific dielectric interaction (π^*) strongly affects the solute. Also, the equation indicates that HBD (α) has a greater effect than HBA (β) for $\tilde{\nu}_a$ and $\tilde{\nu}_f$, whereas, in $\Delta\tilde{\nu}$, the HBD (α) influence is less than that of HBA (β).

It can be noted in Table 4, that the dipole moment of the excited state was greater than ground state dipole moment with all methods. The Kawski–Chamma–Viallet equation gives the determination of ground state and excited state dipole moments. Using the Lippert–Mataga method the excited state dipole moment was estimated in the 10 solvents, the values are nearly equal to those from the Kawski–Chamma–Viallet method, this indicates significant electronic rearrangement of the probe by using the E_T^N method. We obtained dipole difference value of (2.405) using 8 solvents [59]. This indicates that the Lippert–Mataga method may not account for the specific interactions between solute and solvent molecules. It was found that solvent polarity and polarizability played important roles in the solvatochromic studies of 2BME.

Table 5 Mulliken atomic charges (a.u) and electron density (a.u) of the 2BME molecule in vacuum and ethanol calculated using DFT/B3LYP/6-311 and TDDFT/B3LYP/6-311 methods

Atom	DFT/B3LYP (in vacuum)		TDDFT/B3LYP (in ethanol)	
	Electron density	Atomic charge	Electron density	Atomic charge
1 C	6.175301	-0.175301	6.190029	-0.190029
2 C	6.096015	-0.096015	6.108274	-0.108274
3 C	6.210216	-0.210216	6.212495	-0.212495
4 C	5.731672	0.268328	5.732683	0.267317
5 C	6.043765	-0.043765	6.060744	-0.060744
6 C	6.195517	-0.195517	6.193690	-0.193690
7 C	5.483920	0.516080	5.471095	0.528905
8 O	8.484246	-0.484246	8.486323	-0.486323
9 C	6.274832	-0.274832	6.290689	-0.290689
10 O	8.339091	-0.339091	8.387616	-0.387616
11 O	8.480159	-0.480159	8.499185	-0.499185
12 C	6.253597	-0.253597	6.269003	-0.269003
13 C	5.799339	0.200661	5.777201	0.222799
14 C	6.016320	-0.016320	6.013977	-0.013977
15 C	5.868805	0.131195	5.859370	0.140630
16 O	8.493942	-0.493942	8.513951	-0.513951
17 C	6.308176	-0.308176	6.320663	-0.320663
18 C	5.491001	0.508999	5.473997	0.526003
19 C	5.868186	0.131814	5.865773	0.134227
20 C	6.109450	-0.109450	6.118691	-0.118691
21 C	6.129503	-0.129503	6.133109	-0.133109
22 C	6.147192	-0.147192	6.163080	-0.163080
23 C	6.135687	-0.135687	6.146753	-0.146753
24 C	6.154623	-0.154623	6.166039	-0.166039
25 C	6.140157	-0.140157	6.150608	-0.150608
26 C	6.197266	-0.197266	6.200703	-0.200703
27 O	8.352046	-0.352046	8.427377	-0.427377
28 H	0.810394	0.189606	0.792024	0.207976
29 H	0.802332	0.197668	0.796404	0.203596
30 H	0.802365	0.197635	0.797466	0.202534
31 H	0.815452	0.184548	0.807508	0.192492
32 H	0.844338	0.155662	0.822609	0.177391
33 H	0.845078	0.154922	0.817285	0.182715
34 H	0.795256	0.204744	0.772876	0.227124
35 H	0.849901	0.150099	0.823089	0.176911
36 H	0.845237	0.154763	0.823680	0.176320
37 H	0.835540	0.164460	0.812267	0.187733
38 H	0.788923	0.211077	0.779369	0.220631
39 H	0.834610	0.165390	0.807752	0.192248
40 H	0.813058	0.186942	0.801213	0.198787
41 H	0.764291	0.235709	0.786417	0.213583

Table 5 continued

Atom	DFT/B3LYP (in vacuum)		TDDFT/B3LYP (in ethanol)	
	Electron density	Atomic charge	Electron density	Atomic charge
42 H	0.786578	0.213422	0.763677	0.236323
43 H	0.786620	0.213380	0.763248	0.236752

3.3 Quantum Chemical Analysis

The DFT and TDDFT [51] analysis explore the electronic geometry to explain the empirical results. The solvent effectiveness in ethanol was analyzed by PCM, which is a SCR technique [60, 61] using Gamess. The atomic charges and electron densities of 2BME give an idea of the dipole moment and distribution of charges. Electron density and Mulliken atomic charges are listed in Table 5 and plotted in Fig. 10. The atomic charges in vacuum were calculated in the previous study [62]. In vacuum C_1 , C_2 , C_3 , C_4 , C_6 , C_9 and all oxygen atoms have negative charges (donor atoms) whereas all hydrogens are positive, as are C_{12} , C_{19} , C_{15} , C_{13} , C_7 (acceptor atoms). In the ethanol solvent, an increase in the atomic charges of all the atoms is observed; the charges are presented in Table 5. The charge distribution represents the existence of strong polar nature, directing towards the O_{11} ($Q = -0.480$) atom. Such a charge transfer is the characteristic that gives the dipole moment difference between the μ_g and μ_e states. It is noted that TDDFT/B3LYP indicates

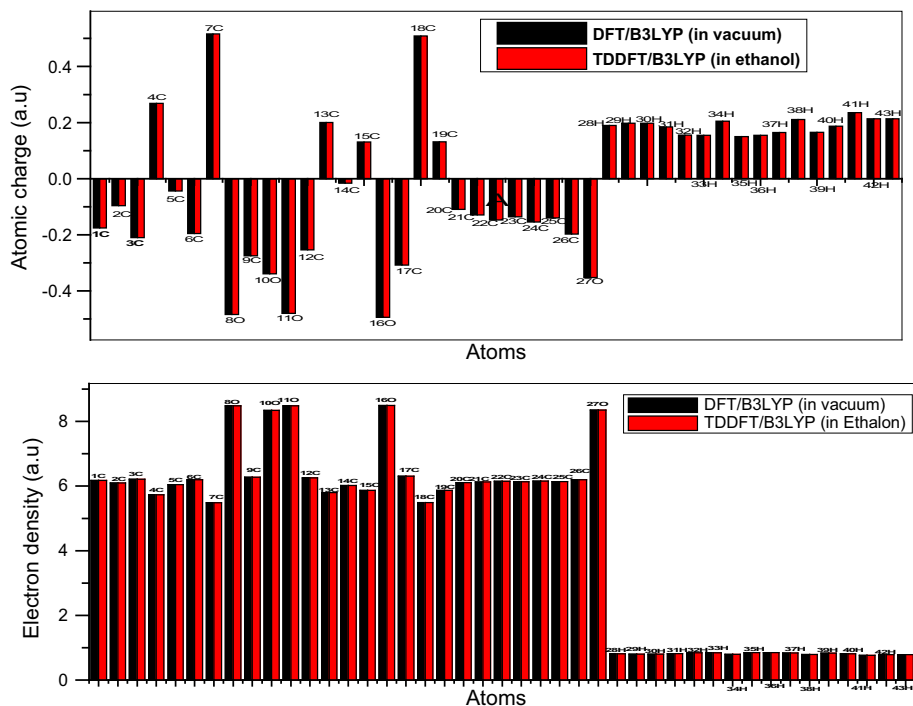


Fig. 10 Calculated atomic charge and electron densities of the 2BME molecule by using DFT/B3LYP/6-311 (d,p) and TDDFT/B3LYP/6-311 (d,p) methods in vacuum and ethanol

an increase in atomic charges because of the inductive effect of the solvent. The change in hydrogen atom gives increased positive values showing charge transfer from hydrogen to the other atoms.

An atomic charge represents the amount of electron cloud situated on an atom and the values of the electron density (8 a.u.) on oxygen atoms are in the order $O(16) > O(8) > O(11) > O(4) > O(5)$. The solvent medium effect tends to decrease the electron cloud of $O(16)$ atom due to p-bond of $O(15)$, whereas there is an increase in the electron cloud of the other oxygen atoms and $C(17)$ has the highest electron density (6.308 Å). HOMO and LUMO analysis give the facts about charge transfer within the molecule. Usually, molecular chemical activity can be understood from the HOMO and LUMO energy gap. The smaller the energy gap and the more easily HOMO electrons can be excited to the LUMO levels. The HOMO and LUMO energies are calculated to be -0.2280 and -0.0800 eV in vacuum and -0.2290 and -0.0814 eV in ethanol, respectively. The difference in energy of LUMO–HOMO in vacuum is slightly more than in ethanol solvent with the value of 0.0004 eV, this

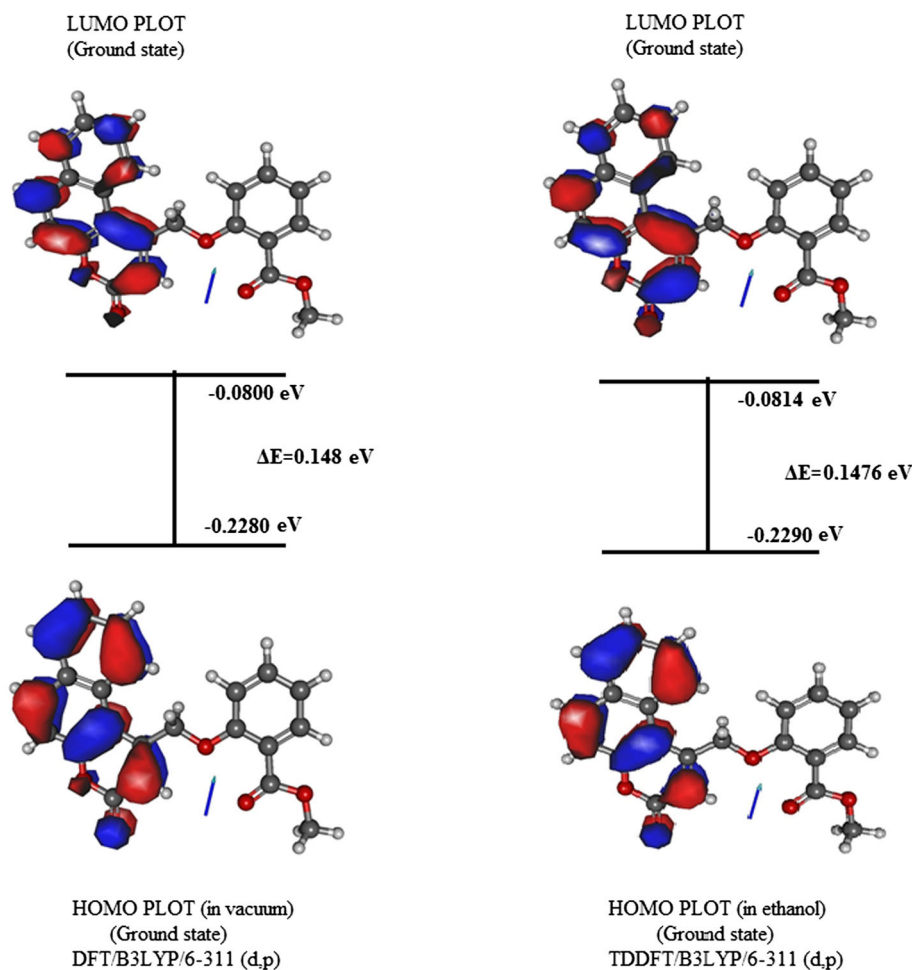


Fig. 11 3D plots of HOMO and LUMO calculated by DFT and TDDFT in vacuum and ethanol for the 2BME molecule

represents the stabilization energy of ethanol. In the LUMO and the HOMO 3D plot, the positive (red) and the negative (green) phases are presented in Fig. 11, which are not corrected for the methyl moiety. In the HOMO topology, density is found to be localized across the double bonds in the aromatic rings. In the LUMO the charge density is not localized across double bonds but is prominently across the single bonds in the aromatic ring; even in the LUMO charge density is found to be absent in the methyl moiety.

The SAS relative to atomic colors and electron densities are shown in Fig. 12a and b. As can be seen from Fig. 12a, SAS is mapped by MEP from charges in the light green regions indicating the interaction of hydrogen atoms in the solvent, the highest region is in the greenish mat yellow zone showing the interaction of hydrogen atoms and medium. It is observed that the interaction of 2BME and medium is controlled predominately by the hydrogen atoms and electron density surface presented in Fig. 12 matches this data.

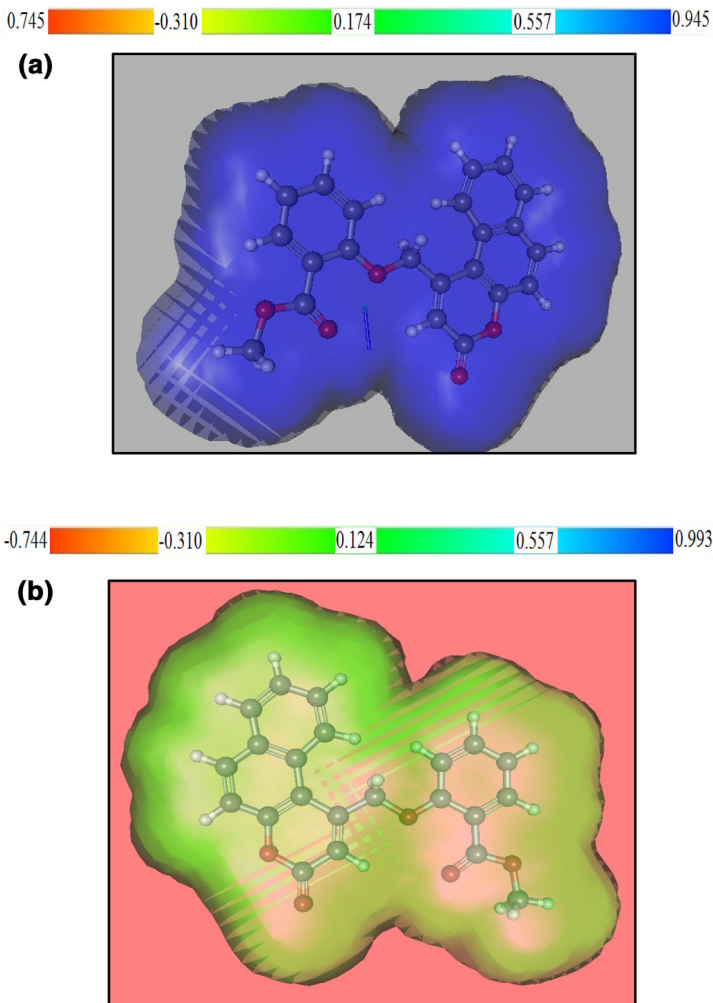


Fig. 12 Solvent accessible surfaces according to atomic charges of the 2BME molecule **a** in vacuum and **b** in ethanol solvent

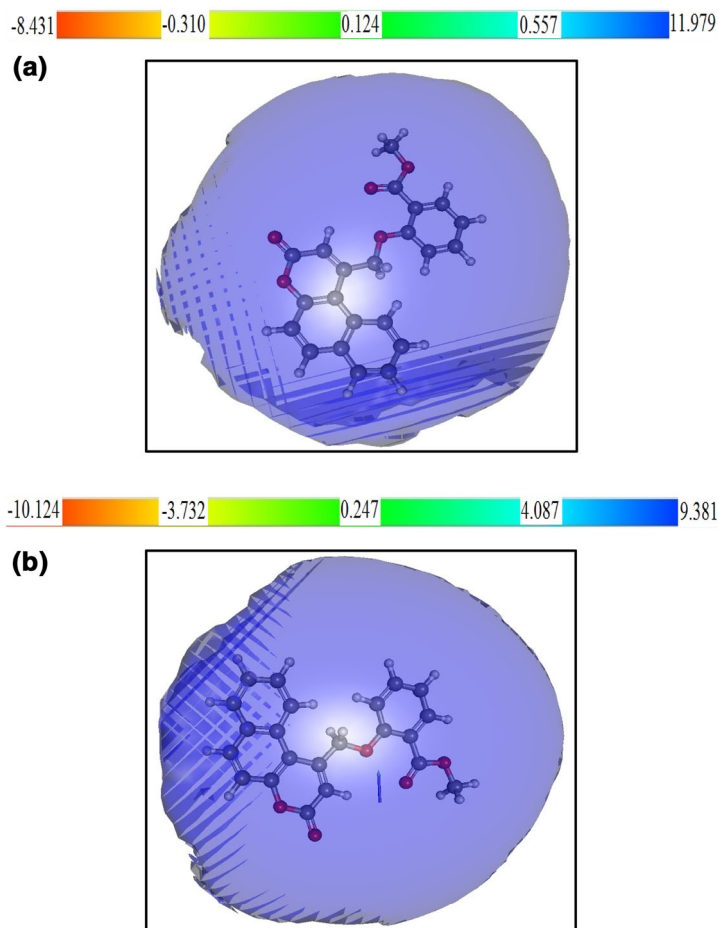


Fig. 13 3D plot of molecular electrostatic potential of 2BME molecule **a** in vacuum and **b** in ethanol solvent

The MEP (Fig. 13) displays the constant electron density surface and helps in obtaining the position for electrophilic, hydrogen bonding interaction and nucleophilic reactions in solvent [63, 64]. Electrostatic potentials at the surface are shown in various colors. The negative charge (red) area of MEP corresponds to electrophilic reactivity and the positive (blue) area represents nucleophilic reactivity (Fig. 13a). The MEP area, the negative cloud which represents surrounding oxygen atoms is not observed and positive regions of potential are observed above the atoms of hydrogen.

4 Conclusions

We obtained the μ_g state by using the Bakshive, Kawski-Chamma method and μ_e state by adopting Kawski-Chamma-Viallet, Bakshieve's, Lippert-Mataga, E_T^N and McRae solvatochromic shift techniques. It is found that μ_e is greater than μ_g . This indicates that the

molecule is more polar in the excited state than in the ground state, which shows the molecule is sensitive to solvent effects. The absorption and emission data have been studied using solvent parameters. Density functional theory B3LYP/6-311(dp) calculations were carried out. The calculated result shows that the optimized geometry can well reproduce the molecular structure. The MEP map shows that the negative and positive potential positions are on electronegative atoms which are around the atoms. These positions provide the data about the regions from where the molecule can have intermolecular interactions. DFT-TDDFT calculations represents that the 2BME molecule is reactive in interacting with the ethanol medium.

Acknowledgements The author Y.F. Nadaf thankful to University Grant Commission New Delhi, India, for financial assistance. YFN thankful to Dr. G. Sriprakash, MSCW for fruitful discussion. Also thankful are Mohamed Zikriya and Pramod A.G. Research Scholars Bangalore University, Bengaluru.

References

1. Puttaraju, K.B., Shivashankar, K., Mahendra, M.C., Rasal, V.P., Vivek, P.N.V., Rai, K., Chanu, M.B.: Microwave assisted synthesis of dihydrobenzo[4,5]imidazo[1,2-*a*]pyrimidin-4-ones; synthesis, *in vitro* antimicrobial and anticancer activities of novel coumarin substituted dihydrobenzo[4,5]imidazo[1,2-*a*]pyrimidin-4-ones. *Eur. J. Med. Chem.* **69**, 316–322 (2013)
2. Bouckaert, C., Serra, S., Rondelet, G., Dolusic, E., Wouters, J., Dogne, J.M., Frederick, R., Pochet, L.: Synthesis, evaluation and structure–activity relationship of new 3-carboxamide coumarins as FXIIa inhibitors. *Eur. J. Med. Chem.* **110**, 181–194 (2016)
3. Farley, C.M., Dibwe, D.F., Ueda, J.Y., Hall, E.A., Awale, S., Magolan, J.: Evaluation of synthetic coumarins for antiausterity cytotoxicity against pancreatic cancers. *Med. Chem. Lett* **26**, 1471–1474 (2016)
4. Ali, M.Y., Jannat, S., Jung, H.A., Choi, R.J., Roy, A., Choi, J.S.: Anti-Alzheimer’s disease potential of coumarins from *Angelica decursiva* and *Artemisia capillaris* and structure–activity analysis. *Asian Pac. J. Trop. Med* **9**, 103–111 (2016)
5. Wei, W., Wu, X.W., Deng, G.G., Yang, X.W.: Anti-inflammatory coumarins with short- and long-chain hydrophobic groups from roots of *Angelica dahurica* cv. Hangbaizhi. *Phytochem* **123**, 58–68 (2016)
6. Thakur, A., Singla, R., Jaitak, V.: Coumarins as anticancer agents: a review on synthetic strategies, mechanism of action and SAR studies. *Eur. J. Med. Chem.* **101**, 476–495 (2015)
7. Abdelhamid, H.N., Wu, H.F.: A method to detect metal–drug complexes and their interactions with pathogenic bacteria via graphene nanosheet assist laser desorption/ionization mass spectrometry and biosensors. *Anal. Chim. Acta* **751**, 94–104 (2012)
8. Abdelhamid, H.N., Khan, M.S., Wu, H.-F.: Design, characterization and applications of new ionic liquid matrices for multifunctional analysis of biomolecules: A novel strategy for pathogenic bacteria biosensing. *Anal. Chim. Acta* **823**, 51–60 (2014)
9. Matagai, N., Kaifu, Y., Koizumi, M.: Solvent effects upon fluorescence spectra and the dipole moment of the excited molecules. *Bull. Chem. Soc. Jpn.* **29**, 465–470 (1956)
10. Chemla, D.S., Zyss, J.: Non-linear optical properties of organic molecules and crystals. Academic Press, New York (1987)
11. Haley, L.V., Hameka, H.F.: Calculation of molecular electric polarizabilities and dipole moments. II. The LiH molecule. *Int. J. Quantum Chem.* **11**, 733–741 (1977)
12. Nadaf, Y.F., Deshpande, D.K., Karguppikar, A.M., Inamdar, S.R.: Estimation of excited state dipole moments of exalite dyes by solvatochromic shift studies. *J. Photosci.* **9**, 29–32 (2002)
13. Nadaf, Y.F., Mulimani, B.G., Inamdar, S.R.: Ground and excited state dipole moments of some exalite UV laser dyes from solvatochromic method using solvent polarity parameters. *J. Mol. Struct. Theorchem.* **678**, 177–181 (2004)
14. Raikar, U.S., Renuka, C.G., Nadaf, Y.F., Mulimani, B.G.: Steady-state, time-resolved fluorescence polarization behaviour and determination of dipole moments of coumarin laser dye. *J. Mol. Struct.* **787**, 127–130 (2006)
15. Raikar, U.S., Renuka, C.G., Nadaf, Y.F., Mulimani, B.G., Karguppikar, A.M., Soudagar, M.K.: Solvent effects on the absorption and fluorescence spectra of coumarins 6 and 7 molecules: Determination of ground and excited state dipole moment. *Spectrochim. Acta A* **65**, 673–677 (2006)

16. Katritzky, A.R., Fara, D.C., Yang, H., Tamm, K., Tamm, T., Karelson, M.: Quantitative measures of solvent polarity. *Chem. Rev.* **104**, 175–198 (2004)
17. Thipperudrappa, J.: Study of solvent effect in 2,5-dpapmc dye using different solvent polarity parameters and estimation of dipole moments. *Mapana. J. Sci.* **14**, 103–119 (2014)
18. Guadarrama, P., Teran, G., Ramos, E., Gutierrez, J., Hernandez, M.: Novel push–pull dendrons with high excited state dipole moments. Synthesis and theoretical analysis of unusual branched electron distribution. *J. Mol. Struct.* **1086**, 17–24 (2015)
19. Joshi, S., Kumara, S., Bhattacharjee, R., Sarmah, A., Sakhuja, R., Pant, D.D.: Experimental and theoretical study: determination of dipole moment of synthesized coumarin–triazole derivatives and application as turn off fluorescence sensor: High sensitivity for iron(III) ions. *Sensors Actuators B: Chem.* **220**, 1266–1278 (2015)
20. El-Daly, S.A.; Alamry, K.A.: Spectroscopic investigation and photophysics of a D- π -A- π -D type styryl pyrazine derivative. *J. Fluoresc.* **26**, 163–176 (2016)
21. Joshi, S., Pant, D.D.: Solvatochromic shift and estimation of dipole moment of quinine sulfate. *J. Mol. Liq.* **166**, 49–52 (2012)
22. Sidir, I., Sidir, Y.G.: Solvent effect on the absorption and fluorescence spectra of 7-acetoxy-6-(2,3-dibromopropyl)-4,8-dimethylcoumarin: determination of ground and excited state dipole moments. *Spectrochim. Acta A* **102**, 286–296 (2013)
23. Zakerhamidi, M.S., Ahmadi Kandjani, S., Moghadam, M., Ortyl, E., Kucharski, S.: Substituent and solvent effects on the dipole moments and photophysical properties of two azo sulfonamide dyes. *J. Mol. Struct.* **996**, 95–100 (2011)
24. Gilani, G., Hosseini, S.E., Moghadam, M., Alizadeh, E.: Excited state electric dipole moment of Nile blue and brilliant cresyl blue: A comparative study. *Spectrochim. Acta A* **89**, 231–237 (2012)
25. Lackowicz, J.R.: *Principles of Fluorescence Spectroscopy*. Plenum Press, New York (1983)
26. Mataga, N., Kaiifu, Y., Koizumi, M.: Solvent effects upon fluorescence spectra and the dipole moment of the excited molecules. *Bull. Chem. Soc. Jpn.* **29**, 465–470 (1956)
27. Kamlet, M.J.: An examination of linear solvation energy relationships. *Prog. Phys. Org. Chem.* **13**, 485–492 (1982)
28. Kamlet, M.J., Abboud, J.L.M., Taft, R.W.: The solvatochromic comparison method. 6. The π^* scale of solvent polarities. *J. Am. Chem. Soc.* **99**, 6027–6035 (1977)
29. Kamlet, M.J., Abboud, J.L.M., Abraham, M.H., Taft, R.W.: Linear solvation energy relationships. A comprehensive collection of the solvatochromic parameters, π^* , α , and β , and some methods for simplifying the generalized solvatochromic equation. *J. Org. Chem.* **48**, 2877–2887 (1983)
30. Bakshiev, N.G.: Universal intermolecular interactions and their effect on the position of the electronic spectra of molecules in two component solutions. *Opt. Spectrosc.* **16**, 821–832 (1964)
31. Kowski, A.: Effect of polar molecules on electronic spectrum on 4-amino-phthalimide. *Acta Phys. Polon.* **25**, 285–290 (1964)
32. Kowski, A.: Abnormal Stokes shift of the absorption and of the fluorescence maximum of 4-aminophthalimide in dioxane–water mixtures. *Acta Phys. Polon.* **28**, 647–652 (1965)
33. Kowski, A., Stefanowska, U.: The anomalous red shift of the absorption and fluorescence spectra of 4-aminophthalimide in dependence on the ratio of homo- and heteropolar solvents. *Acta Phys. Polon.* **28**, 809–822 (1965)
34. Kowski, A., Kołakowski, W.: Über die temperaturabhängigkeit der absorptions—und fluoreszenzspektren von 4-amino-phthalimid. *Acta Phys. Polon.* **29**, 177–186 (1966)
35. Kowski, A., Pasztor, B.: Elektrische dipolmomente von N-phenyl- α -naphthylaminimgrund-und anregungszustand. *Acta Phys. Polon.* **29**, 187–193 (1966)
36. Chamma, A., Viallet, P.: Determination du moment dipolaire d'une molecule dans un etat excite singulet. *Sci. Paris Ser. C* **270**, 1901–1904 (1970)
37. Reichardt, C., Welton, T.: *Solvents and solvent effects in organic chemistry*. Wiley-VCH Verlag GmbH and Co, weinheim (2010)
38. Sidir, I., Sidir, Y.G.: Estimation of ground and excited state dipole moments of oil red O by solvatochromic shift methods. *Spectrochim. Acta A* **135**, 560–567 (2015)
39. Boregowda, P., Kalegowda, S., Rasal, V.P., Reddy, J., Koyye, J.E.: Synthesis and biological evaluation of 4-(3-hydroxy-benzofuran-2-yl)coumarins. *Org. Chem. Int* **2014**, 1–7 (2014)
40. Reichardt, C.: *Solvents and Solvent Effects in Organic Chemistry*. VCH, New York (2005)
41. Lide, D.R. (ed.): *Handbook Chemistry and Physics*, 76th edn. CRC Press, Boca Raton (1995)
42. Lide, D.R. (ed.): *Handbook Chemistry and Physics*, 80th edn. CRC Press, New York (1999)
43. Reichardt, C., Ratajczak, H., Orville-Thomas, W.J. (eds.): *Molecular Interactions*, vol. 3. John Wiley and Sons Ltd, New York (1982)

44. Lippert, E.: Spektroskopische bestimmung des dipole moment saromatischer verbindungen im ersten angereigten singulettzustand. *Z Electrochem* **6**, 962–975 (1957)
45. Bakshiev, N.G.: Universal intermolecular interactions and their effect on the position of the electronic spectra of molecules in two component solutions. *Opt. Spektrosk.* **16**, 821–832 (1964)
46. Chamma, A., Viallet, P.: Determination du moment dipolaire d'une molecule dans un etat excite singulet. *Comptes Rendus Acad. Sci. Paris Ser. C* **270**, 1901–1908 (1970)
47. McRae, E.G.: Theory of solvent effects on molecular electronic spectra frequency shifts. *J. Phys. Chem.* **61**, 562–572 (1957)
48. Edward, J.T.: Molecular volumes and parachor. *Chem. Ind.* **30**, 774–777 (1956)
49. Reichardt, C.: Solvents and Solvent Effects in Organic Chemistry. VCH, Weinheim (1988)
50. Kamlet, M.J., Abboud, J.L.M., Taft, R.W.: An examination of linear solvation energy relationships. *Prog. Phys. Org. Chem.* **13**, 485–630 (1981)
51. Schmidt, M.W., Baldrige, K.K., Boatz, J.A., Elbert, S.T., Gordon, M.S., Jensen, J.H., Koseki, S., Matsunaga, N., Nguyen, K.A., Su, S., Windus, T.L., Dupuis, M., Montgomery, J.A.: General atomic and molecular electronic structure system. *J. Comput. Chem.* **14**, 1347–1363 (1993)
52. Pramanik, S., Banerjee, P., Sarkar, A., Mukherjee, A., Mahalanabis, K.K., Bhattacharya, S.C.: Spectroscopic investigation of 3-pyrazolyl 2-pyrazoline derivative in homogeneous solvents. *Spectrochim. Acta A* **71**, 1327–1332 (2008)
53. Willard, D.M., Riter, R.E., Levinger, N.E.: Dynamics of polar solvation in lecithin/water/cyclohexane reverse micelles. *J. Am. Chem. Soc.* **120**, 4151–4160 (1998)
54. Saha, S., Samanta, A.: Influence of the structure of the amino group and polarity of the medium on the photophysical behavior of 4-amino-1,8-naphthalimide derivatives. *J. Phys. Chem. A* **106**, 4763–4771 (2002)
55. Lippert, E.: Spektroskopische bistimmung des dipolmomentes aromatischer verbindugen im ersten angeregten singulettzustand. *Z Electrochem* **61**, 962–975 (1957)
56. Kamlet, M.J., Taft, R.W.: The solvatochromic comparison method. The α -scale of solvent hydrogen-bond donor (HBD) acidities. *J. Am. Chem. Soc.* **98**, 377–383 (1976)
57. Nagarajan, V., Brearley, A.M., Kang, T., Barbara, P.F.: Time-resolved spectroscopic measurements on microscopic solvation dynamics. *J. Chem. Phys.* **86**, 3183–3196 (1987)
58. Kahlow, M.A., Kang, T.J., Barbara, P.F.: Transient solvation of polar dye molecules in polar aprotic solvent. *J. Chem. Phys.* **86**, 2372–2378 (1988)
59. Khattab, M., Van Dongen, M., Feng Wang, F., Clayton, A.H.A.: Solvatochromism and linear solvation energy relationship of the kinase inhibitor SKF86002. *Spectrochim. Acta A* **170**, 226–233 (2017)
60. Wong, M.W., Frisch, M.J., Wiberg, K.B.: Solvent effects the mediation of electrostatic effects by solvents. *J. Am. Chem. Soc.* **113**, 4476–4782 (1991)
61. Cancès, E., Mennucci, B., Tomasi, J.: A new integral equation formalism for the polarizable continuum model: theoretical background and applications to isotropic and anisotropic dielectrics. *J. Chem. Phys.* **107**, 3032–3041 (1997)
62. Sidir, I., Gulseven Sidir, Y., Kumalar, M., Tasal, E.: Ab initio Hartree-Fock and density functional theory investigations on the conformational stability, molecular structure and vibrational spectra of 7-acetoxy-6-(2,3-dibromopropyl)-4,8-dimethylcoumarin molecule. *J. Mol. Struct.* **964**, 134–151 (2010)
63. Scrocco, E., Tomasi, J.: Electronic molecular structure, reactivity and intermolecular forces: an euristic interpretation by means of electrostatic molecular potentials. *Adv. Quantum Chem.* **11**, 115–198 (1979)
64. Luque, F.J., Lopez, J.M., Orozco, M.: Perspective on electrostatic interactions of a solute with a continuum. A direct utilization of ab initio molecular potentials for the prevision of solvent effects. *Theor. Chem. Acc.* **103**, 343–345 (2000)